IL NUOVO CIMENTO **41 C** (2018) 140
DOI 10.1393/ncc/i2018-18140-6

COLLOQUIA: LaThuile 2018

Mixing and CP violation in charm at LHCb

L. HENRY on behalf of the LHCb COLLABORATION
IFIC - Valencia, Spain

received 6 September 2018

Summary. — Violation of the charge-parity (CP) symmetry has been observed in several systems (kaons, $B_{d,s}$ mesons), all of which are related to the down-quark sector. It remains to be observed in the up-quark sector, where only the c quark manifests flavour oscillations. The LHCb experiment is now playing a major role in charm physics. This document reviews some of the latest results on charm physics from LHCb, specifically on the measurement of CP asymmetries in the $D^{\pm}_{(s)} \to \eta'\pi^{\pm}$ and $\Lambda_c^+ \to ph^+h^-$ channels, as well as the most precise measurement of mixing and CP-violation (CPV) parameters with $D^0 \to K\pi$ decays.

1. – Introduction

In the Standard Model (SM), CP violation (CPV) effects arise from the interference between several amplitudes. An example of processes where CPV is expected to happen is singly Cabibbo-suppressed decays, such as $\Lambda_c^+ \to pK^+K^-$ or $\Lambda_c^+ \to p\pi^+\pi^-$, where the Cabibbo-suppressed tree amplitude competes with a loop diagram. As a result, physical observables measured in such diagrams are potentially sensitive to the addition of new physics (NP) particles inside of the loop. It is also possible to have CPV effects due to the interference between mixing and decay, and such CPV could also be sensitive to NP.

CPV effects in the charm sector of the SM are typically suppressed by a $(1/m_c)$ factor. However, NP coupling solely to the up-quark sector could enhance these effects [1]. Current limits and measurement of CPV in the charm sector are compatible with the SM description.

The LHCb experiment [2] is now playing a major role in charm physics, thanks to the large sample of c-hadrons recorded ($\mathcal{O}(10^7)$). It is a single-arm forward spectrometer covering the pseudorapidity range $2 < \eta < 5$, originally designed for the study of particles containing b or c quarks. The detector is composed of a silicon-strip vertex detector surrounding the pp interaction region that allows c- and b-hadrons to be identified from their typically long flight distance, and a tracking system that provides a measurement of the momentum of charged particles by the measurement of track parameters upstream and downstream from a magnet. In addition, particle identification is provided

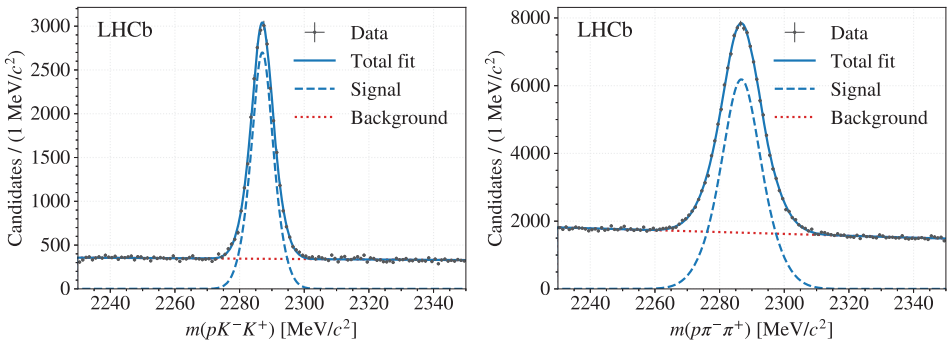

Fig. 1. – Invariant-mass distributions in the pK^+K^- (left) and $p\pi^+\pi^-$ (right) final states, selected by semileptonic decays. The solid line corresponds to the total fit, with the signal being represented by the dashed, blue line and the combinatorial background by dotted, red lines [3].

by two ring-imaging Cherenkov detectors on the two sides of the magnet. Finally, electromagnetic and hadron calorimeters, located upstream the muon stations, complete the detector. In the Run I (2010–2012) of the LHC, the LHCb experiment collected $3\,\text{fb}^{-1}$ of integrated luminosity at two different energies of 7 TeV ($1\,\text{fb}^{-1}$) and 8 TeV ($2\,\text{fb}^{-1}$). While in the current Run II (2015–2018), about $3.8\,\text{fb}^{-1}$ has been collected since 2015 at a centre-of-mass energy of 13 TeV.

2. – ΔA_{CP} in $\Lambda_c^+ \to pK^+K^-$ and $\Lambda_c^+ \to p\pi^+\pi^-$ decays (Run I) [3]

The $\Lambda_c^+ \to pK^+K^-$ and $\Lambda_c^+ \to p\pi^+\pi^-$ are two singly Cabibbo-suppressed baryon decays. As a result, potentially sizeable CPV effects can arise in the interference between tree- and loop-level diagrams. As both modes are selected as part of the $\Lambda_b^0 \to \Lambda_c^+\mu^-X$ decay chain, the raw asymmetry of a decay to a flavour-eigenstate $f\mu^-$ is calculated from measured yields as

$$A_{\text{raw}}(f) = \frac{N(f\mu^-) - N(\overline{f}\mu^+)}{N(f\mu^-) + N(\overline{f}\mu^+)}, \tag{1}$$

and is related to A_{CP} through

$$A_{\text{raw}}(f) = A_{CP} + A_{\text{production}} + A_{\text{detection}}(f), \tag{2}$$

where the two last terms, respectively the production and detection asymmetries, are a potential large source of systematic errors. These two terms can be cancelled in the measurement of a difference in A_{CP} between two modes, or ΔA_{CP}, provided that the kinematical differences are taken into account. A fit is performed on the $\Lambda_c^+ \to ph^+h^-$ invariant-mass distributions in order to extract signal yields, as shown in fig. 1.

As the production and detection asymmetries depend on kinematics, a reweighting is used to match the kinematical distributions. Most notably, the underlying dynamics of the two decays are different, as illustrated by their Dalitz plot distribution, shown in fig. 2. The $\phi(1020)$ contribution dominates the pKK amplitude, whereas multiple resonances compete in the $p\pi\pi$ mode. It is chosen to use the $p\pi\pi$ kinematics as a reference.

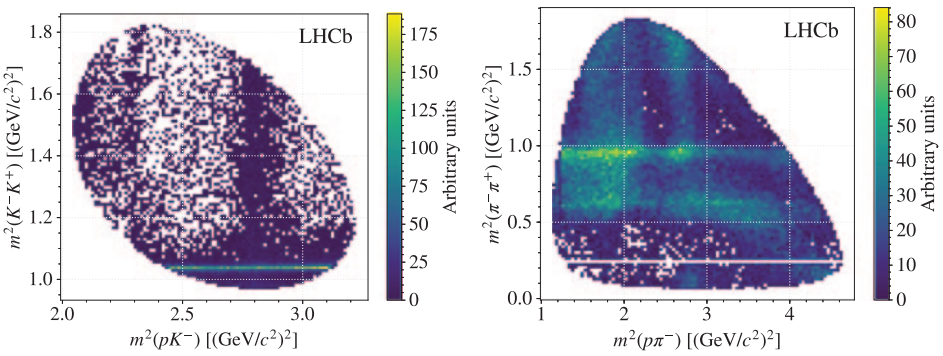

Fig. 2. – Dalitz plot distribution of data in the $\Lambda_c^+ \to pK^+K^-$ (left) and $\Lambda_c^+ \to p\pi^+\pi^-$ (right) modes [3].

After reweighting, the raw *CP* asymmetries are measured to be

$$A_{\rm raw}(pK^+K^-) = (3.72 \pm 0.78)\%, \tag{3}$$

$$A_{\rm raw}(p\pi^+\pi^-) = (3.42 \pm 0.47)\%, \tag{4}$$

corresponding to

$$\Delta A_{CP} = (0.30 \pm 0.91 \pm 0.61)\%, \tag{5}$$

where the first uncertainties are statistical and the second are systematic. The measurement is statistically limited, and the main systematic uncertainties arise from the size of the simulated samples.

Additionally, the large statistics available allows to perform this measurement splitting years and magnet polarities, in order to cross-check the method. As shown in fig. 3, all the partial measurements are compatible. This is the first measurement of a *CP* parameter in a 3-body Λ_c^+ decay.

3. – *CPV* in $D^\pm \to \eta'\pi^\pm$ and $D_s^\pm \to \eta'\pi^\pm$ decays (Run I) [4]

The study of charm decays to pseudoscalar mesons allows to constrain amplitudes between different modes through triangle relations, or to shed light on the $SU(3)$ symmetry breaking. The $D^\pm \to \eta'\pi^\pm$ and $D_s^\pm \to \eta'\pi^\pm$ decays are both singly Cabibbo-suppressed decays, with topologies similar to the Cabibbo-favoured modes $D^\pm \to K^0_S\pi^\pm$ and $D_s^\pm \to \phi\pi^\pm$, respectively. *CP* asymmetries in the two latter, Cabibbo-favoured modes have been measured with a 10^{-3} precision, making them excellent control modes [5, 6].

In order to perform cross-checks, the sample is split into three parts, depending on the trigger requirement. A first sample (T1) requires that the trigger is fired by an energy deposit in the hadronic calorimeter by a decay particle. The sample T2 is formed by events where the trigger is fired from such an energy deposit by an unrelated particle. Finally, events in the sample T3 are triggered by an energy deposit in the electromagnetic calorimeter from an unrelated particle or a high-p_T muon.

Signal candidates are extracted from a fit to the $\eta'\pi^\pm$ invariant-mass spectrum, which corresponds to roughly 6.3×10^4 and 1.5×10^5 candidates for the D and Ds modes,

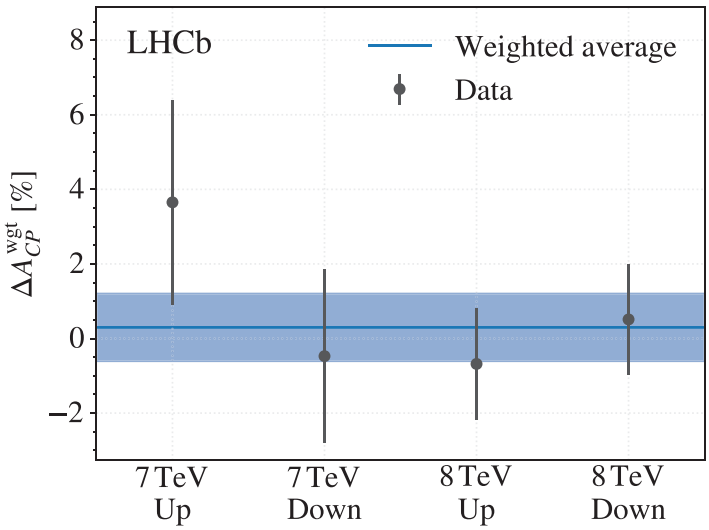

Fig. 3. – Measured values for ΔA_{CP} between the $\Lambda_c^+ \to pK^+K^-$ and $\Lambda_c^+ \to p\pi^+\pi^-$ modes, split by centre-of-mass energies and magnet polarities. The blue line and shaded area correspond to the weighted average and its uncertainty, respectively [3].

respectively. In order to match the kinematics of the signal and control modes, fits are performed in nine bins of (p_T, η) as shown in fig. 4, and the measured raw asymmetries are combined using a weighted average.

The results show no dependence on the trigger category and on the centre-of-mass energy, as shown in fig. 5, and the ΔA_{CP} are measured to be

$$\Delta A_{CP}(D^\pm \to \eta'\pi^\pm) = (-0.58 \pm 0.72 \pm 0.53)\%, \tag{6}$$

$$\Delta A_{CP}(D_s^\pm \to \eta'\pi^\pm) = (-0.44 \pm 0.36 \pm 0.22)\%, \tag{7}$$

where the first and second uncertainties are statistical and systematic, respectively. Considering the currently measured A_{CP} of the control modes, this corresponds to

$$A_{CP}(D^\pm \to \eta'\pi^\pm) = (-0.61 \pm 0.72 \pm 0.53 \pm 0.12)\%, \tag{8}$$

$$A_{CP}(D_s^\pm \to \eta'\pi^\pm) = (-0.82 \pm 0.36 \pm 0.22 \pm 0.27)\%, \tag{9}$$

where the last uncertainty is due to the measured A_{CP} values of the control modes.

4. – Charm mixing and *CPV* with $D^0 \to K\pi$ decays (Run I and Run II) [7]

Flavour oscillations in the D^0-$\overline{D}^0$ system were first evidenced by the BaBar and Belle Collaborations [8, 9], and were measured for the first time in a single experiment by LHCb [10]. It has been measured in the $D^0 \to K\pi$ channel through the interference between the doubly Cabibbo-suppressed decay $D^0 \to K^+\pi^-$ channel and an oscillation, followed by the Cabibbo-favoured $\overline{D}^0 \to K^-\pi^+$ decay. This update of the analysis uses

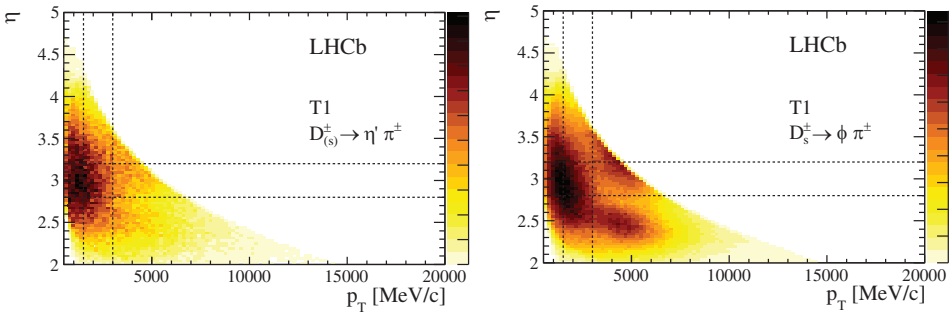

Fig. 4. – Distributions of (p_T, η) in the T1 trigger category for candidates in the $\eta'\pi^{\pm}$ final state (left) and for $D_s^{\pm} \to \phi\pi^{\pm}$ control mode candidates (right). Dashed lines indicate the limits of bins chosen to perform the reweighting [4].

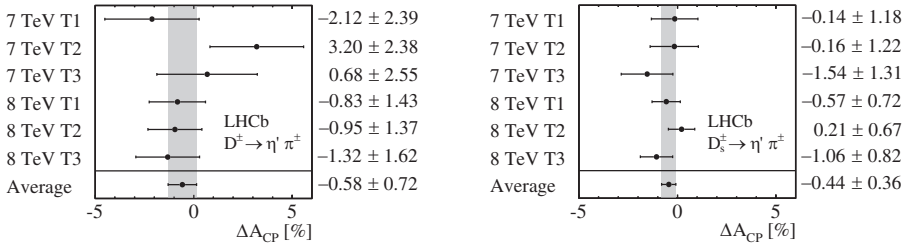

Fig. 5. – Measured ΔA_{CP} values for $D^{\pm} \to \eta'\pi^{\pm}$ (left) and $D_s^{\pm} \to \eta'\pi^{\pm}$ (right), split by centre-of-mass energy and trigger category. The shaded area corresponds to the weighted average [4].

the full Run I dataset along with data from 2015 and 2016. It aims at measuring the time-dependent ratios of suppressed-to-favoured decay rates, approximated as

$$R^{\pm}(t) = R_D^{\pm} + \sqrt{R_D^{\pm}} y'^{\pm} t + \frac{(x'^{\pm})^2 + (y'^{\pm})^2}{4} t^2, \tag{10}$$

where the $+(-)$ index refers to a decay from a D^0 ($\overline{D}^0$) and R_D is the ratio between decay amplitudes considering only the tree-level diagrams. The two terms x' and y' are defined as

$$x' = x\cos(\delta) + y\sin(\delta), \tag{11}$$

$$y' = y\cos(\delta) - x\sin(\delta), \tag{12}$$

where $x = \Delta m/\Gamma$ and $y = \Delta\Gamma/2\Gamma$ are the D^0 oscillation parameters, and δ is the strong-phase difference between the suppressed and favoured amplitudes, as measured by the CLEO-c and Belle Collaborations [11,12]. Any difference between the x', y' or R_D measured for D^0 and $\overline{D}^0$ would signal CPV in the charm sector. CPV associated with a difference in R_D would be associated with "direct" CPV, whilst differences between x' or y' values depending on flavour would indicate CPV in the interference between mixing and decay.

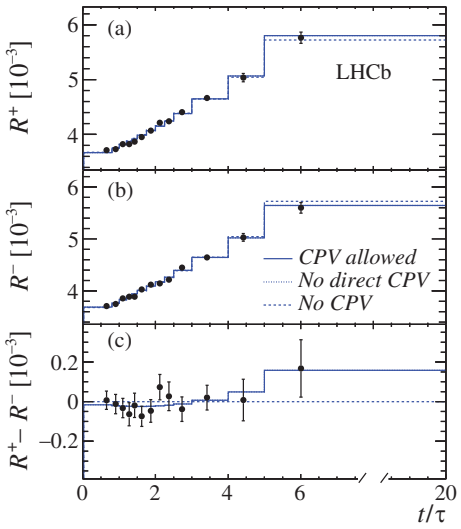

Fig. 6. – Binned fits to the lifetime distributions of R^+ (top), R^- (middle), and $R^+ - R^-$ (bottom). The solid, blue line indicates the fit where CPV is allowed, the dotted, blue line the fit where only indirect CPV is allowed, and the dashed, blue line the fit where no CPV is allowed [7].

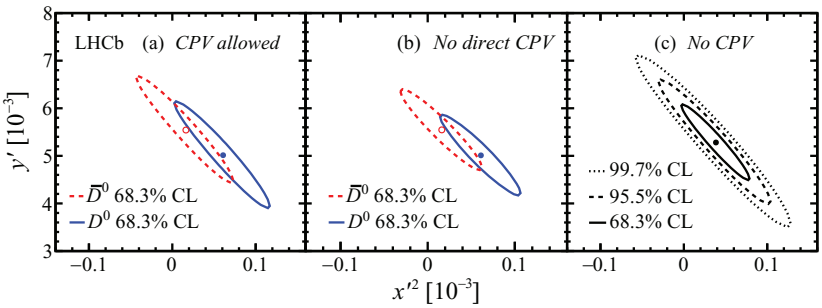

Fig. 7. – Resulting contours on the $(x'^2 - y')$ plane allowing CPV (left), only allowing indirect CPV (middle), and disallowing CPV (right). On the two first plots, the ellipse corresponding to D^0 ($\overline{D}^0$) is plotted in solid, blue (dashed, red) line [7].

The $R^{\pm}$ observable is measured in 13 bins of lifetime, whose boundaries are chosen so as to minimise uncertainties. Several fits are performed, allowing for no CPV, only indirect CPV, and no CPV. Figure 6 shows the result of these fits, and fig. 7 shows the resulting contours on the (x'^2-y') plane. The results are consistent with an absence of CPV.

5. – Conclusion

Recent results on the measurement of mixing and CPV parameters in the charm sector by the LHCb experiment have been reviewed. All are consistent with SM expectations. The results presented here are only a part of the activity devoted to charm physics in

the LHCb experiment. For instance, recent results that are not covered include the measurement of CP asymmetries in the $D^0 \to K^+K^-$ decay [13], the measurement of A_Γ in the $D^0 \to K^+K^-$ and $D^0 \to \pi^+\pi^-$ decays [14], and the search for CPV in the phase space of $D^0 \to \pi^+\pi^-\pi^+\pi^-$ decays [15]. These analyses profit from the wealth of experience gathered analysing Run I datasets. Additionally, some of them are already in the "upgrade era", as they run directly their Run II analysis on the output of the trigger ("turbo trigger"). Finally, the systematic use of control modes, consistency checks, and adequate observables allows to keep systematic errors under control. As such, despite huge datasets, $\mathcal{O}(10^5$–$10^7)$ signal candidates, all presented measurements are still statistically limited.

REFERENCES

[1] Grossman Y., Kagan A. L. and Nir Y., *Phys. Rev. D*, **75** (2007) 036008.
[2] LHCb Collaboration (Alves Jr. A. A. *et al.*), *JINST*, **3** (2008) S08005.
[3] Aaij R. *et al.*, *JHEP*, **03** (2018) 182.
[4] Aaij R. *et al.*, *Phys. Lett. B*, **771** (2017) 21.
[5] Belle Collaboration (Ko B. R. *et al.*), *Phys. Rev. Lett.*, **109** (2012) 021601.
[6] Belle Collaboration (Won E. *et al.*), *Phys. Rev. Lett.*, **107** (2011) 221801.
[7] Aaij R. *et al.*, *Phys. Rev. D*, **97** (2018) 031101.
[8] Aubert B. *et al.*, *Phys. Rev. Lett.*, **98** (2007) 211802.
[9] Starič M. *et al.*, *Phys. Rev. Lett.*, **98** (2007) 211803.
[10] LHCb Collaboration (Aaij R. *et al.*), *JHEP*, **2012** (2012) 129.
[11] Onyisi P. U. E. *et al.*, *Phys. Rev. D*, **88** (2013) 032009.
[12] Won E. *et al.*, *Phys. Rev. Lett.*, **107** (2011) 221801.
[13] LHCb Collaboration (Aaij R. *et al.*), *Phys. Lett. B*, **767** (2017) 177.
[14] Aaij R. *et al.*, *Phys. Rev. Lett.*, **118** (2017) 261803.
[15] LHCb Collaboration (Aaij R. *et al.*), *Phys. Lett. B*, **769** (2017) 345.